Journal of Medicinal Chemistry

Article

pubs.acs.org/jmc

Discovery of Diverse Human Dihydroorotate Dehydrogenase Inhibitors as Immunosuppressive Agents by Structure-Based Virtual Screening

Yanyan Diao,† Weiqiang Lu,† Huangtao Jin, Junsheng Zhu, Le Han, Minghao Xu, Rui Gao, Xu Shen, Zhenjiang Zhao, Xiaofeng Liu, Yufang Xu, Jin Huang,* and Honglin Li*

State Key Laboratory of Bioreactor Engineering, Shanghai Key Laboratory of New Drug Design, Shanghai Key Laboratory of Chemical Biology, School of Pharmacy, East China University of Science and Technology, Shanghai 200237, China

Supporting Information

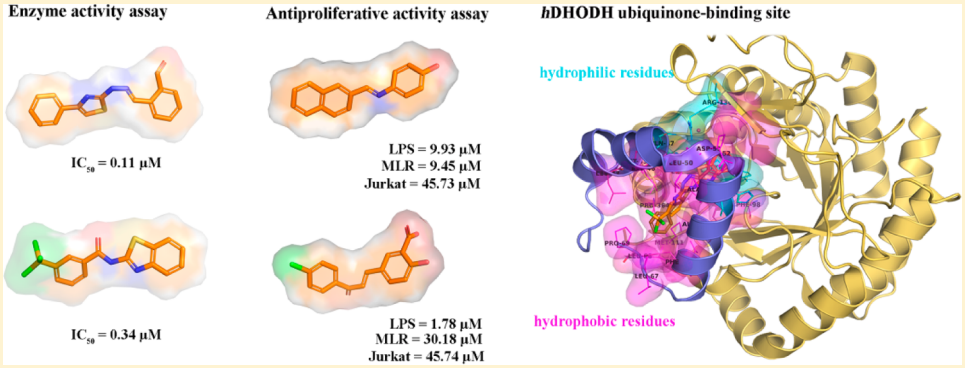

ABSTRACT: This study applied an efficient virtual screening strategy integrating molecular docking with MM-GBSA rescoring to identify diverse human dihydroorotate dehydrogenase (*h*DHODH) inhibitors. Eighteen compounds with IC_{50} values ranging from 0.11 to 18.8 μM were identified as novel *h*DHODH inhibitors that exhibited overall species-selectivity over *Plasmodium falciparum* dihydroorotate dehydrogenase (*pf*DHODH). Compound **8**, the most potent one, showed low micromolar inhibitory activity against *h*DHODH with an IC_{50} value of 0.11 μM. Moreover, lipopolysaccharide-induced B-cell assay and mixed lymphocyte reaction assay revealed that most of the hits showed potent antiproliferative activity against B and T cells, which demonstrates their potential application as immunosuppressive agents. In particular, compound **18** exhibited potent B-cell inhibitory activity (IC_{50} = 1.78 μM) and presents a B-cell-specific profile with 17- and 26-fold selectivities toward T and Jurkat cells, respectively.

INTRODUCTION

Human dihydroorotate dehydrogenase (*h*DHODH) is anchored on the inner membrane of mitochondria and can be categorized as a class 2 DHODH, the electron receptors of which are mainly respiratory ubiquinones.[1] On the other hand, class 1 DHODHs, which exist chiefly in prokaryotes, are located in the cytosolic membrane and use diverse water-soluble molecules, such as fumarate and nicotinamide adenine dinucleotide, as redox cofactors.[2] As an essential enzyme that catalyzes the oxidation of DHO to orotate, DHODH plays a critical role in de novo pyrimidine biosynthesis of DNA and RNA production. Moreover, DHODH is essential to rapidly proliferating cells, such as tumor cells as well as stimulated T and B cells,[3−5] which makes it an attractive target for the treatment of cancer, rheumatoid arthritis, and many other autoimmune diseases. Recent studies have shown that the suppression of mitochondrial DHODH could induce p53 stress response, indicating its great potential for the treatment of tissue damage.[6] In addition, by depleting pyrimidine pools to suppress viral RNA synthesis, DHODH inhibitors present a broad spectrum of antiviral activity, thereby allowing for the development of antiviral agents.[7,8]

The structure of class 2 DHODHs can be divided into two parts: the N-terminal domain containing two α-helices and the C-terminal domain comprising a large α/β barrel.[9] In *h*DHODH, there are binding sites for the substrate DHO, the cofactors flavin mononucleotide and ubiquinone. Research has confirmed that small molecule inhibitors abrogate the activity of *h*DHODH by displacing either DHO or the cofactor ubiquinone from the corresponding binding site.[10] To date, various inhibitors against *h*DHODH have been reported for the treatment of cancer as well as autoimmune and inflammatory diseases,[11−13] among which leflunomide **1** and brequinar **3** are the most successful ones. Compound **1** is a prodrug converted to an active metabolite A771726 **2** in the gut and liver,[14] and it

Received: May 7, 2012
Published: September 17, 2012

is now being marketed for the treatment of rheumatoid arthritis. As a potent *h*DHODH inhibitor, it could also enhance therapeutic responses in melanoma cells both in vitro and in mouse *xenograft* models,[15] whereas compound **3** is mainly used for the treatment of cancer and graft-versus-host disease. However, the clinical applications of both compounds **1** and **2** are not highly satisfactory because of diverse side effects. Administration of compound **1** for an extended period may cause unexpected severe adverse reactions, such as hypertension and interstitial lung disease,[16,17] whereas compound **3** has a narrow therapeutic window that significantly limits its clinical use.[18−20] Consequently, the need to identify novel *h*DHODH inhibitors as therapeutic agents by blocking pyrimidine biosynthesis for the treatment of cancer as well as autoimmune and inflammatory diseases persists.[21]

Chart 1. Selected Structures of the Reported *h*DHODH Inhibitors Which Have Been Confirmed To Bind in the Ubiquinone-Binding Pocket

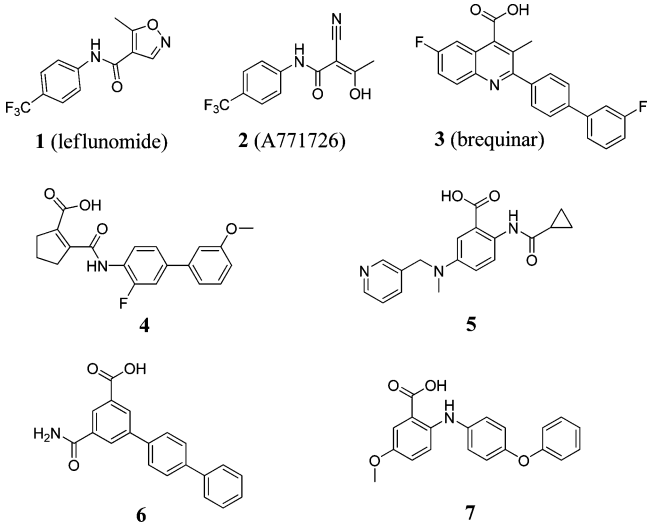

Liu et al. first reported the three-dimensional crystal structures of *h*DHODH in complex with compound **2** and an analogue of compound **3**, both of which occupied the N-terminal domain, a tunnellike ubiquinone-binding site.[22] As many crystal structures of *h*DHODH in complex with inhibitors have been reported in the literature, it is feasible to discover new *h*DHODH inhibitors using structure-based virtual screening technology,[23] which is capable of predicting the interaction modes between proteins targets and their ligands. In this study, 18 novel compounds with IC_{50} values ranging from 0.11 to 18.8 μM that exhibited an overall species-selectivity over *Plasmodium falciparum* dihydroorotate dehydrogenase (*pf*DHODH) were identified as *h*DHODH inhibitors via hierarchical structure-based virtual screening. These compounds offer novel scaffolds that establish a solid foundation for uncovering new DHODH regulatory mechanisms. In addition, most of the hits showed in vitro antiproliferative activities against B and T cells, suggesting their potential application as immunosuppressive agents.

EXPERIMENTAL SECTION

Protein Preparation. The crystal structure of *h*DHODH in complex with an analogue of **3** (PDB code: 1D3G) was derived from Protein Data Bank.[24] Hydrogen atoms and charges were added during a brief relaxation performed using the "Protein Preparation Wizard" workflow in Maestro 9.0 (Schrödinger LLC).[25] All HETATM residues and crystal water molecules were removed except the inhibitor and a crucial water molecule (W444) which bridges the interaction between the inhibitor and binding site by a hydrogen bond. After the hydrogen bond network was optimized, the crystal structure was minimized until the root-mean-square deviation (rmsd) between the minimized structure and the starting structure reached 0.3 Å with OPLS 2005 force field.

Glide Docking. Molecular docking study was performed using Glide (Schrödinger LLC).[26,27] The grid-enclosing box was placed on the centroid of the binding ligand in the optimized crystal structure as described above and defined to enclose residues located within 14.0 Å of the ubiquinone-binding site, and a scaling factor of 1.0 was set to van der Waals (VDW) radii of those receptor atoms with partial atomic charges of less than 0.25. After addition of hydrogen atoms and ionization at a pH range from 5.0 to 9.0, the stereoisomers and the 3D conformers of compounds in SPECS database (~280000 compounds)[28] were generated with the Ligprep module.[29] Standard precision (SP) and extra precision (XP) approaches of Glide were respectively adopted to dock the molecules into the ubiquinone-binding site with the default parameters, and the top-ranking poses of each molecule were retained. After Glide SP scoring, the top 5000 docking poses were reserved and subjected to XP calculation with a more precise scoring function, and the top 1000 docking poses were retained for subsequent calculation with MM-GBSA approach.

Prime/MM-GBSA. The docking poses obtained from Glide calculation were taken as the input for Prime/MM-GBSA calculation with default parameters,[30] which is used to predict the free binding energy for various sets of ligands against a receptor. Ligand strain energy and protein flexibility were not taken into account, and the poses of compounds generated by Glide XP were relaxed and minimized using the local optimization feature in the Prime module.[31] The energies were estimated by the OPLS-AA force field for molecular mechanics energy (E_{MM}) and the surface-generalized born model for polar solvation energy (G_{SGB}), and a nonpolar solvation term (G_{SA}) was also included. The binding free energy (ΔG_{bind}) was calculated as follows:

$$G = E_{MM} + G_{SGB} + G_{SA}$$
$$\Delta G_{bind} = G_{complex} - (G_{protein} + G_{ligand}) \quad (1)$$

The top 300 compounds ranked by Prime/MM-GBSA were reserved for further visual observation.

Similarity Analysis and Cluster. To measure the diversity and novelty of the top 300 compounds reranked by Prime/MM-GBSA method, Tanimoto coefficient (Tc) values of chemical similarity were calculated for each pair of compounds among the 300 candidates and the 7 known *h*DHODH inhibitors (compounds **1**−**7**) using SciTegic extended-connectivity fingerprints (ECFP_4) in Pipeline Pilot 7.5.[32] ECFP_4 is an atom type-based method, and the neighbor atoms within a diameter of four bonds are considered when calculating the features for each atom.[33] On the basis of the Tanimoto similarity metric, the 307 compounds were clustered into 20 groups using the maximum dissimilarity method of Pipeline Pilot 7.5 with default parameters. After visual inspection by considering the docking poses and structural diversity and novelty, 47 candidates out of the 300 compounds were purchased and tested in the *h*DHODH inhibitory activity assay.

Chemistry. All compounds were commercially available and purchased from SPECS, and the purities were determined by HPLC using an Agilent 1200-series instrument equipped with a Diamonsil-C18 column (250 × 4.6 mm, 5 μm particle size) and a UV/vis detector setting of λ = 254 nm. All compounds were eluted with two solvent systems (CH_3CN as organic phase in Method I and CH_3OH as organic phase in Method II) as listed in Table S1 (Supporting Information) at a flow rate of 1 mL/min unless otherwise specified. HPLC analysis of the compounds assayed confirmed the purity at ≥95%.

DHODH Enzyme Activity Assay. The expression vectors for human and *Plasmodium falciparum* DHODH were kindly provided by

Prof. Jon Clardy (Harvard Medical School). Both of the two enzymes were expressed and purified as described previously.[22,34] DHODH activities were tested by monitoring the reduction of 2,6-dichloroindophenol (DCIP) as reported previously.[35] The assay mixture contained 25 nM DHODH, 50 mM HEPES (pH 8.0), 0.15 M KCl, 100 μM CoQ_0, and 100 μM DCIP. Stock solutions of compounds were prepared in DMSO and were diluted using the assay buffer solution. A 180 μL solution of DHODH enzyme in assay buffer was incubated with 10 μL of various concentrations of compound solutions for 10 min. The reaction was initiated by adding 10 μL of dihydroorotate for a final concentration of 500 μM and recording the decrease in absorbance at 600 nm for 5 min on a Synergy 2 Multi-Mode Microplate Reader (BioTek, Winoosi, VT). Compound **2** was used as a positive control, and the IC_{50} values were determined with three independent determinations.

Spleen Proliferation Assay. To investigate the immunosuppressive effects of *h*DHODH inhibitors, the antiproliferative activities on mouse spleen cells of these compounds have been determined. The Spleen proliferation assay was performed as described previously.[36] Spleen cells from ICR mice were collected by squeezing the spleen through eight layers of gauze and centrifuged at 1000*g* for 10 min. Pellets were added to an erythrocyte lysis buffer (0.17 M Tris-HCl, 0.75% NH_4Cl pH 7.5), and the mixture was subjected to centrifugation to remove the erythrocytes. Splenocytes were cultured at a density of 5×10^5 cells/well in 96-well plates in RPMI 1640 medium and stimulated by 10 μg/mL of lipopolysaccharide (*Escherichia coli* 055:B5, Sigma) in the presence of compounds at an indicated concentration. After incubation for 72 h, the cells were further incubated with 20 μL of 5 mg/mL MTT for 4 h at 37 °C in a humidified incubator with 5% CO_2. Then the formazan crystals were dissolved in 150 μL of DMSO, and the absorbance was measured at 570 nm by using a Synergy 2 Multi-Mode Microplate Reader (BioTek). The IC_{50} values were determined from the results of three independent experiments and calculated from the inhibition curves.

Mixed Lymphocyte Reaction (MLR). The two-way mouse mixed lymphocyte reaction was performed according to standard procedures.[37] Briefly, spleen cells of C57BL/6 and BALB/C were separated as described above. Each set of 2×10^5 cells were incubated in 96-well cell culture plates with a serial dilution of compounds in 200 μL of RPMI 1640 medium containing 10% FBS gentamicin (Gibco) and 50 μM β-mercaptoethanol (Sigma). Stock solutions of all compounds were prepared in DMSO and diluted in RPMI 1640 medium for the assay. After 4 days of incubation, the cells were further incubated with 20 μL of 5 mg/mL MTT for 4 h at 37 °C in a humidified incubator with 5% CO_2. Then the formazan crystals were dissolved in 150 μL of DMSO, and the absorbance was measured at 570 nm by using a Synergy 2 multimode microplate reader (BioTek, Winooski, VT). The effects of compounds on cell proliferation were assessed by subtracting the proliferation of BALB/6 spleen cells alone as background from all the values. The IC_{50} values were determined from the results of at least three independent tests and calculated from the inhibition curves.

Cell Toxicity Assay. To investigate the lymphocyte cells toxicity of *h*DHODH inhibitor, we utilized a human T-cell line Jurkat to estimate the antiproliferative activity. An amount of 2×10^5 Jurkat cells in RPMI medium were seeded in 96-well plates in the absence or presence of compounds at the indicated concentration. The cell viability is detected using MTT method as described above.

RESULTS AND DISCUSSION

The putative ubiquinone-binding site was chosen for virtual screening of new *h*DHODH inhibitors based on the crystal structure of *h*DHODH in complex with an analogue of compound **3** (PDB code: 1D3G). The entrance of the channellike pocket is surrounded by a large hydrophobic helical domain that is presumed to be involved in the membrane association, and several hydrophilic residues exist at the end of the pocket (Figure 1A). W444, a conservatively buried water molecule observed frequently in several cases of

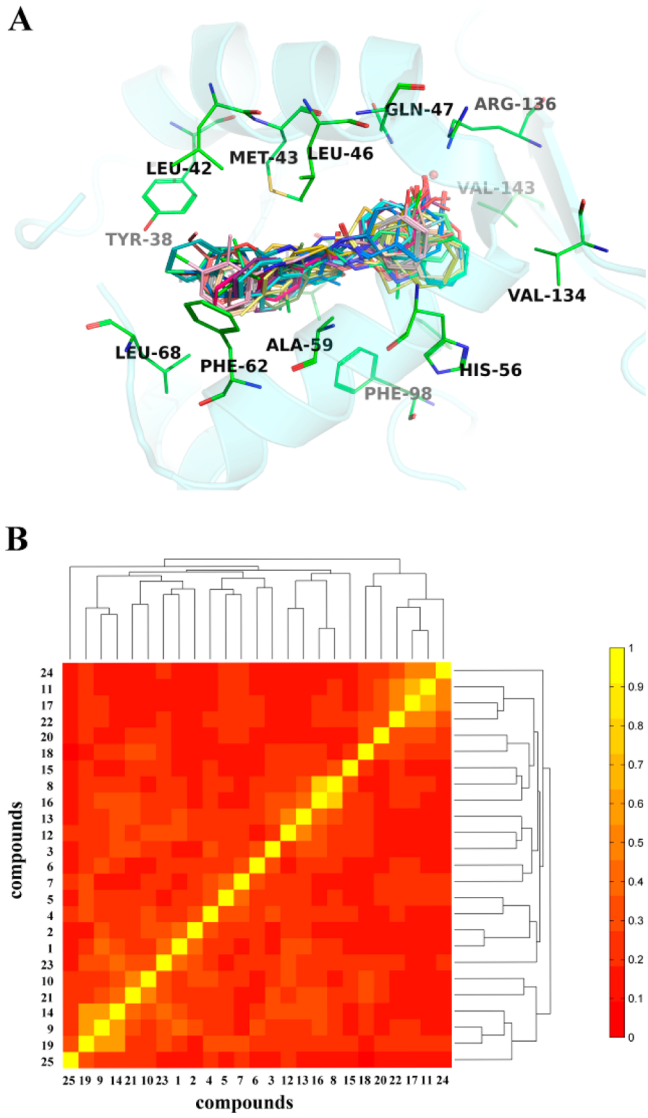

Figure 1. Characteristics of the 18 *h*DHODH inhibitors in chemical structures and predicted binding poses. (A) Superimposition of the docking poses of inhibitors in the ubiquinone-binding site. (B) Heatmap presentation of topological similarities of the 18 hits to the 7 reported *h*DHODH inhibitors.

*h*DHODH–ligand complexes,[11,22,38−40] which mediated the hydrogen-bond interactions between the protein and its inhibitors, was reserved in the protein preparation process for further virtual screening. After hierarchical virtual screening was implemented with Glide docking and Prime/MM-GBSA rescoring (Figure S1, Supporting Information), 300 top-ranking compounds were retrieved as candidates from the SPECS database. The candidates were then clustered using molecular similarity evaluation to reduce their structural redundancy. With consideration of key interactions observed from the crystal structures, such as van der Waals (VDW) complementarity and some notable hydrogen bonds with polar residues Gln47, Arg136, and W444, each docked pose of these candidates was carefully checked manually by visual inspection to remove those that are likely to be nonbinders.[41] Moreover, we presumed that, apart from appropriate functional groups that significantly affect binding affinity, the sizes of compounds are also important factors that deserve more attention; for instance, only those compounds with hydrophobic tails buried

dx.doi.org/10.1021/jm300630p | J. Med. Chem. 2012, 55, 8341−8349

in the pocket were considered. Of 47 compounds finally selected and purchased for experimental bioassay testing, 18 (with a hit rate of 38.3%) were identified as *h*DHODH inhibitors with IC_{50} values ranging from 0.11 to 18.8 μM (Table 1), and compound **8** exhibited considerable inhibitory potency compared with compound **2**, which served as the control.

To investigate which scoring function is more suitable for identifying novel *h*DHODH inhibitors, we plotted GlideXP scores and Prime/MM-GBSA scores (Table 1) against experimental pIC_{50} values for the 18 active compounds (Figure 2). The results showed that there is no correlation between the GlideXP scores and experimental pIC_{50} values (R^2 = 0.13). However, based on the good-quality binding modes proposed using Glide with XP precision, an encouraging correlation between the Prime/MM-GBSA score and experimental data was obtained (R^2 = 0.71), which outperformed the GlideXP results by demonstrating more accurate prediction of binding affinities. Moreover, of the 18 hits obtained using the Prime/MM-GBSA approach, only 5 were ranked by Glide XP docking in the top 300 candidates (Table S2, Supporting Information), which also revealed the enrichment ability of Prime/MM-GBSA for the discovery of novel active compounds. The better performance of Prime/MM-GBSA in ranking the potential ligands, which has been validated in many other protein−ligand systems, may be ascribed to its more realistic treatment of solvation effects,[42] because most reactions of biological interest occur in water.[43] The successful combination of Glide score for the generation of binding poses and Prime/MM-GBSA for the prediction of binding affinities also indicated its suitability for predicting *h*DHODH−ligand binding affinity as well as its promising application for further *h*DHODH discovery and subsequent structural optimization of the described hits.

The aims of this study were to find new and diverse *h*DHODH inhibitors through virtual screening and to identify novel scaffolds for further lead optimization.[44] Hence, to evaluate the structural novelty of the candidates and remove redundant analogues, we performed molecular similarity assessment and clustering among the 300 top-ranking candidates and the 7 known inhibitors (compounds **1**−**7**). The 300 candidates had a maximum Tc value of 0.49 to the 7 known inhibitors, which exhibited structural novelty as a whole (a Tc cutoff value of 0.5 was set to define similarity). Subsequently, the 307 compounds were clustered into 20 groups, and the candidates were selected or excluded principally by their predicted binding features with *h*DHODH as described above. Meanwhile, the compounds with the same scaffold were reserved with a maximum of three for in vitro enzyme activity assay to maximize the structural diversity. As illustrated in Figure S2, the 47 candidates covered almost all clusters of the 300 candidates. The maximum average Tc value of the topological similarity of the 47 candidates to the 7 known inhibitors and the average Tc value were 0.33 and 0.15, respectively, indicating the novelty of the selected candidates as novel chemotypes. Moreover, for the identified 18 hits, the maximum and average Tc values to the 7 known inhibitors were 0.29 and 0.15, respectively. Compounds **8** and **16** share a common structural scaffold, as do compounds **9**, **14**, and **19**. Except for the former two groups, the *Tc* values were low with predominant scattering below 0.3 for most inhibitor pairs, which indicated that these hits are topologically dissimilar to one another (Figure 1B). Moreover, the results showed that these inhibitors exhibited very similar predicted poses when binding to *h*DHODH (Figure 1A), and their relatively rigid scaffolds, which are mainly composed of aromatic rings, fit well

Table 1. Inhibitory Activities of the Compounds against *h*DHODH and *pf*DHODH in Enzyme Activity Assay and Their GlideXP and MM-GBSA Scores

Compd.	Structure[a]	Scores		IC_{50} (μM)[b]	
		GlideXP	MM-GBSA	*h*DHODH	*pf*DHODH
8	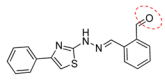	-12.52	-41.88	0.11	NA
9	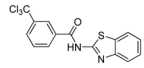	-10.99	-44.95	0.34	1.93
10	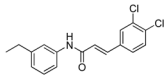	-11.55	-37.56	0.55	NA
11	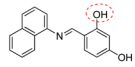	-11.29	-37.46	0.78	NA
12	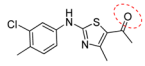	-12.38	-39.52	0.93	0.76
13	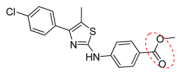	-12.34	-42.77	1.27	NA
14	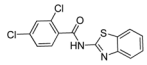	-8.00	-34.53	1.83	4.67
15	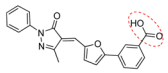	-10.84	-36.71	2.74	NA
16	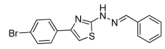	-13.61	-34.30	3.30	NA
17	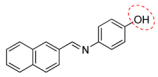	-11.65	-35.67	3.96	NA
18	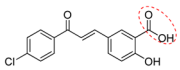	-10.89	-37.21	6.06	NA
19	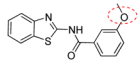	-10.65	-36.42	6.83	NA
20	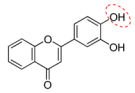	-9.98	-33.47	12.38	9.48
21	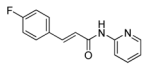	-10.23	-26.51	13.01	NA
22	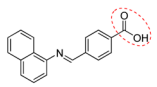	-13.32	-27.24	15.62	NA
23	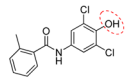	-7.43	-29.47	16.08	NA
24	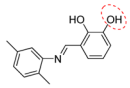	-10.63	-29.05	17.75	NA
25	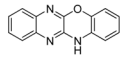	-5.28	-27.12	18.28	NA
2	--	--	--	0.13	11.39

[a]Functional groups involved in hydrogen bond interactions in the putative binding poses are highlighted and labeled. [b]IC_{50} values were determined from the results of at least three independent tests, and attempts to determine IC_{50} values were made if the inhibition rate at 10 μM was larger than 20%. NA indicates no activity in the assay.

dx.doi.org/10.1021/jm300630p | J. Med. Chem. 2012, 55, 8341−8349

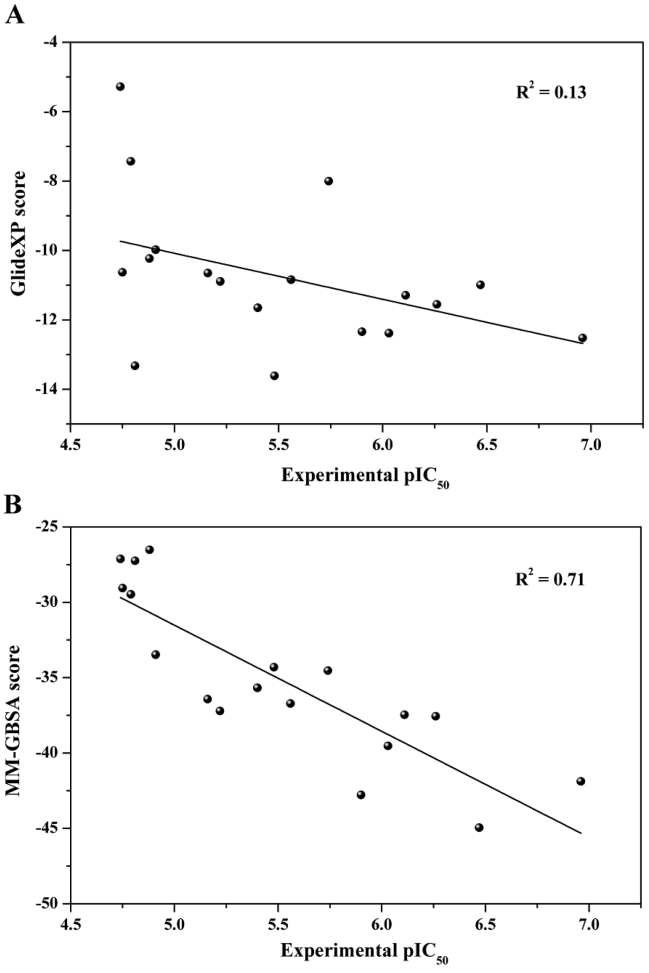

Figure 2. Comparison of the correlation between experimental pIC_{50} values of the 18 hit compounds and corresponding (A) GlideXP scores and (B) MM-GBSA scores.

into the narrow ubiquinone-binding site with similar steric shapes. (To determine whether these compounds bind to the ubiquinone-binding site, we performed kinetic assays with compound **12**, and the results, as depicted in Figure S3, demonstrated that the representative compound **12** is a competitive inhibitor of *h*DHODH with respect to ubiquinone binding). Most of the inhibitors contained hydrogen-bond-forming groups, such as the formyl group of compound **8**, the ester group of compound **13**, and the carboxyl group of **15**, which may form hydrogen bond interactions with the hydrophilic residues Gln47 or Arg136 or the water molecule (W444) in the hydrophilic region of the binding site. However, the hydrogen-bond interactions did not appear to be essential, because significant hydrogen bond interactions were not observed for compounds **9** and **10**, which exhibited low micromolar inhibitory activities against *h*DHODH.

Previously found to be associated with antimicrobial activities,[45,46] compounds **8** and **16** are thiazole derivatives and are first identified as potent *h*DHODH inhibitors by bearing such a structural scaffold. In the proposed binding pose of compound **8** with *h*DHODH, the formyl-substituted phenyl ring is located at the polar end of the ubiquinone-binding pocket. The carbonyl group is hydrogen-bonded to residues Gln47 and Arg136 (Figure 3A), or a hydrogen bond interaction may form between the carbonyl group and the water molecule (W444). The 4-phenylthiazole moiety extends to the entrance of the pocket and fits the pocket well through hydrophobic effects and VDW interactions with residues such as Leu42, Met43, Ala59, Phe62, and Leu359. In the absence of a carbonyl group (a hydrogen bond acceptor), compound **16** displayed an approximately 30-fold weaker inhibitory potency with respect to compound **8**, indicating the great significance of the hydrogen-bond interactions. Similar critical hydrogen-bond interactions with residues Gln47 and Arg136 were also seen in the predicted binding modes of *h*DHODH and many other inhibitors that contained hydrogen-bond-forming groups, and the functional groups involved are highlighted in Table 1.

The amphipathic properties of the *h*DHODH inhibitors described above are congruent with what have been validated with the crystal structures of *h*DHODH in complex with the inhibitors as reported previously.[21] Hydrogen-bond interactions are widely accepted to be crucial for the determination of inhibitory potency against *h*DHODH and should be taken into account in the design and optimization of potential *h*DHODH inhibitors. However, by investigating the predicted binding modes of compounds **9** (IC_{50} = 0.34 μM) and **10** (IC_{50} = 0.55 μM), we found that both potent inhibitors could not match the pharmacophore features because hydrogen-bond interactions were absent (Figure 3B and 3C). The strongly hydrophobic trichloromethyl group of compound **9** is located in the hydrophobic region and extends to the mouth of the pocket formed by the nonpolar residues Tyr38, Met43, Phe62, and Pro364, and the benzo[*d*]thiazole ring points toward residues Val134 and Val143 to putatively participate in favorable hydrophobic and VDW interactions. The 3,4-dichlorophenyl moiety of compound **10** is buried in the polar environment, and the 3-ethylphenyl ring occupies the hydrophobic section of the pocket with the ethyl tail pointing to the cavity formed by residues Leu42, Met43, and Phe62. The location and orientation of compound **14**, which exhibits the 2,4-dichloro substitution pattern on the phenyl ring, are similar to those of compound **9**, whereas compound **19** with methoxy substitution at the 3-position of the phenyl ring binds to *h*DHODH in a different manner with its overall scaffold rotating approximately 180°. Compound **19** can possibly form a hydrogen bond with Arg136 through oxygen atoms (Figure 3D), but it was approximately 20-fold less active than compound **9** in the enzyme activity assay. Notably, for inhibitors without hydrogen-bond interactions with residues Gln47 and Arg136, the inhibitory activities should be attributed to hydrophobic interactions and steric effects, especially the shapes complement against the tunnellike ubiquinone-binding site.

DHODH is a universal enzyme that also exists in the malaria parasite *Plasmodium falciparum*. The malaria parasite relies exclusively on de novo pyrimidine biosynthesis for survival, and *pf*DHODH is also a promising target for small molecule antimalarial therapeutic agents.[47] To continue our study on new potential antimalarial agents[48] and explore the selectivity of the 18 *h*DHODH inhibitors, we analyzed an in vitro enzyme activities assay against *pf*DHODH. As summarized in Table 1, only four compounds exhibited moderate activities against *pf*DHODH with IC_{50} values <10 μM; the other compounds showed very weak potencies with inhibition rates <20% at 10 μM. Although both human and *Plasmodium falciparum* DHODH belong to the family of class 2 DHODHs and share a highly conserved sequence in the α/β barrel domain, the sequences of the ubiquinone-binding N-terminal domain vary greatly between the the two enzymes, which could explain

dx.doi.org/10.1021/jm300630p | J. Med. Chem. 2012, 55, 8341−8349

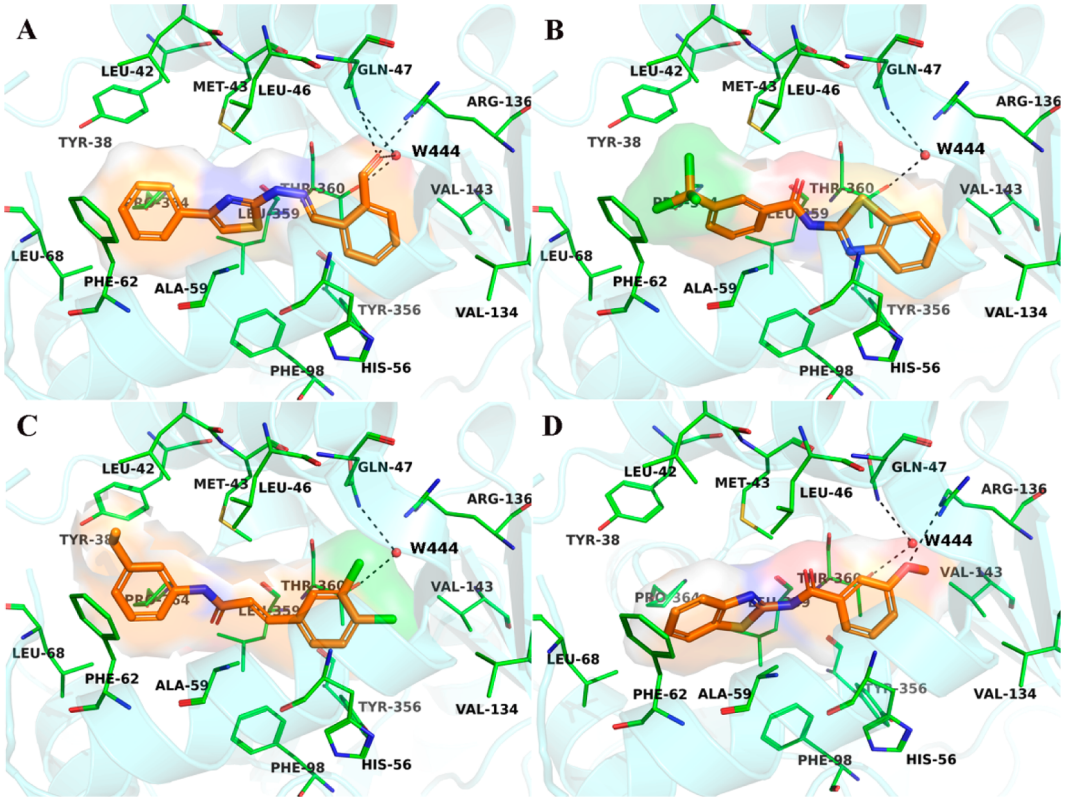

Figure 3. Predicted binding poses of four representative compounds (A) **8**, (B) **9**, (C) **10**, and (D) **19** against *h*DHODH in the ubiquinone-binding pocket. Key residues around the binding pocket are shown as green lines, and the inhibitors are presented as sticks. The reserved water (W444) is depicted as a red ball, and the hydrogen bonds are labeled as black dashed lines.

the potency differences for inhibitors that bind in the pocket. At the entrance of the pocket, residues Leu42 and Pro364 in *h*DHODH are replaced by residues Phe171 and Met536, respectively, in *pf*DHODH, which makes the binding pocket in *pf*DHODH less open. In addition, residues Val134 and Val143 are substituted by larger hydrophobic residues Ile263 and Ile272, respectively, at the end of the pocket in *pf*DHODH, which reduces the overall size of the *pf*DHODH ubiquinone-binding pocket.[49] In the in vitro enzyme activity assay, the IC_{50} value of compound **12** against *pf*DHODH was slightly lower than that against *h*DHODH, and compound **20** exhibited better inhibitory effects against *pf*DHODH than against *h*DHODH. In contrast to compounds **12** and **20**, compounds **9** and **14**, with slightly larger scaffolds, inhibited *pf*DHODH less potently than *h*DHODH, indicating their slightly selective potency against *h*DHODH (Table 1). Much larger potent *h*DHODH inhibitors such as compounds **10**, **13**, and **15** are very poor *pf*DHODH inhibitors, which may be attributed to the size constraints of the smaller *pf*DHODH pocket.

To further probe the structural basis for *pf*DHODH inhibition, the four identified inhibitors were docked into the ubiquinone-binding pocket of *pf*DHODH (PDB code: 3I65) via a GlideXP protocol. The substitutions of Leu172 for Met43 and Phe188 for Ala59 triggered the docking configurations of the four compounds in *pf*DHODH to deviate from their positions in *h*DHODH at the end of the pocket (Figure S4, Supporting Information). Compounds **9**, **12**, and **14** may form hydrogen bonds with His185 (corresponding His56 in *h*DHODH) via their nitrogen atoms on the linkers, and the hydrogen-bond pattern with His185 is considered to be the critical binding feature against *pf*DHODH due to the elimination of hydrogen bonding feasibility with Gln47, which was found in *h*DHODH to be caused by the replacement of Leu176 with Gln47 in *pf*DHODH.[50] An additional hydrogen bond formed between Arg265 (corresponding Arg136 in *h*DHODH) and the carbonyl group of compound **12**, which is the most potent *pf*DHODH inhibitor, albeit a very weakly selective one, based on our result. Compound **20** is a flavone analogue, and one of its hydroxyl groups is probably hydrogen-bonded to Arg265. Despite the absence of a highly species-selective profile against *pf*DHODH, the four compounds may serve as starting scaffolds for further optimization as selective *pf*DHODH inhibitors, and the observed preferential inhibition of the 18 hits also provide helpful clues for new inhibitor development.

Human DHODH is a central enzyme of pyrimidine nucleotide synthesis, and it has been targeted for the treatment of autoimmune diseases, the clinical syndrome caused by the activation of T cells B cells or both in the absence of an ongoing infection or other discernible causes.[51] Compound **1**, a disease-modifying antirtheumatic drug, has been demonstrated to block T-cell proliferation in a dose-dependent manner and induce several functional changes in T cells.[52] Meanwhile, it can inhibit the formation of specific antibodies secreted by B cells.[53] To investigate the immunosuppressive effects of these *h*DHODH inhibitors, we determined the antiproliferative activities on mouse spleen cells of those hits with IC_{50} values <10 μM in the enzyme activity assay. The B-cell and T-cell immunosuppressive activities of the compounds were tested using lipopolysaccharide (LPS)-stimulated mouse spleen cell proliferation and the two-way mouse mixed lymphocyte reaction (MLR), respectively.[54] Lymphocyte cells toxicity was

dx.doi.org/10.1021/jm300630p | *J. Med. Chem.* 2012, 55, 8341−8349

also assessed using the Jurkat T-cell line to estimate their therapeutic window. As shown in Table 2, compound **2** potently suppressed LPS-induced B-cell proliferation with an IC_{50} value of 4.07 μM but exhibited weak inhibitory effects against T-lymphocyte proliferation in MLR with an IC_{50} value of 48.03 μM. Cyclosporin A (CsA), a potent and selective T-cell immunosuppressant with an IC_{50} value of 11 nM, was used as another control. Except for compound **16**, which exhibited intense cytotoxicity with an IC_{50} value of 1.07 μM against the Jurkat cell line, all the tested compounds showed immunosuppressive effects in B-cell proliferation, the MLR assay, or both in varying degrees. Although less potent than CsA, most of our *h*DHODH inhibitors were more potent than compound **2** in the MLR assay. In addition, our compounds presented a profile better than that of CsA in the LPS-induced B-cell proliferation assay. Compounds **8**, **10**, and **17** had comparable inhibitory effects in B-cell proliferation, and their MLRs and activities against Jurkat cells are very weak. Despite the potent inhibitory activities against both B and T cells, compound **12** demonstrated a cytostatic character because it is devoid of selectivity toward Jurkat cells, which may need to be optimized to lower the cytotoxicity in our further study. Compounds **9**, **14**, and **19** are moderate B-cell inhibitors with obvious selectivities toward T and Jurkat cells. Compound **18** is the most potent B-cell inhibitor (IC_{50} = 1.78 μM), and it also exhibits a B-cell-specific profile with 17- and 26-fold selectivities toward T and Jurkat cells, respectively. However, the B-cell immunosuppressive activity of **18** is not likely to completely correlate with enzyme inhibition potency with a higher IC_{50} value of 6.06 μM in the *h*DHODH enzyme assay. It is a more complicated process for cell inhibition, and compound **18** may have effects on other enzymes or biological pathways as well when targeting B-cells, which therefore renders it a valuable tool for the investigation of new targets for B-cell intervention.[55] In addition, for the 18 discovered hits, no obvious correlation was observed between their enzyme inhibition potency and antiproliferative activity. It is also possible that off-target effects emerged and the antiproliferative activity was mediated by action upon other targets. Further biological experiments are ongoing to elucidate the exact antiproliferative activity of the hits.

Table 2. In Vitro Antiproliferative Activities against B Cells and T Cells of *h*DHODH Inhibitors and Reference Compounds[a]

compd	LPS[b]	MLR[c]	Jurkat[d]
8	14.04	12.38	>100
9	8.74	25.38	43.54
10	11.21	8.38	30.13
11	11.32	23.62	26.32
12	4.65	9.58	5.39
13	13.02	13.31	15.74
14	19.85	58.46	>100
15	>100	73.48	>100
16	>100	>100	1.07
17	9.93	9.45	45.73
18	1.78	30.18	45.74
19	16.12	>100	>100
2	4.07	48.03	26.65
CsA	>100	0.011	>10

[a]IC_{50} values were determined from the results of at least three independent tests. IC_{50} values in μM. [b]Inhibition of mouse B-cell proliferation induced by LPS. [c]Inhibition of the two-way mouse mixed lymphocyte reaction. [d]Inhibiton of human T-cell line Jurkat cell proliferation.

CONCLUSION

In summary, 18 potential *h*DHODH inhibitors were identified by hierarchical structure-based virtual screening. Compared with the known *h*DHODH inhibitors (compounds **1**−**7**), the diverse hits discovered in this study possessed novel scaffolds and showed distinct predicted binding features in the ubiquinone-binding pocket to some extent. For the hits containing hydrogen bond-forming groups, hydrogen bond interactions may form with residues Gln47 and Arg136, and these hits used their amphipathic properties to accommodate the pocket. Meanwhile, there were several hits without detectable hydrogen-bond interactions in the hydrophilic region of the pocket, and their inhibitory activities may be attributed to hydrophobic interactions and steric effects, especially the shapes complement against the tunnellike ubiquinone-binding site. The distinct binding modes will help enhance our knowledge of and provide an alternative strategy for the design of new *h*DHODH inhibitors. Moreover, as assessed by LPS-induced B-cell assay and MLR assay, many of the hits exhibited in vitro antiproliferative effects against B and T cells that depended heavily on DHODH for quick proliferation, demonstrating their potential to trigger symptoms of many autoimmune diseases such as rheumatoid arthritis and systemic lupus erythematosus. We believe that the hits discovered in this study will provide new drug candidates for the treatment of autoimmune diseases by targeting B and T cells.

ASSOCIATED CONTENT

Supporting Information

Schematic representation of hierarchical virtual screening strategy, heatmap presentation of hierachical clustering of the 300 top-ranking candidates and the 7 reported *h*DHODH inhibitors, determination of inhibition kinetics of compound **12** against *h*DHODH, a figure showing proposed binding modes of compounds **9**, **12**, **14**, and **20** with *h*DHODH and *pf*DHODH, a table listing HPLC analysis data of the 18 hit compounds, rankings from the GlideXP and Prime/MM-GBSA results, and a table of in silico predicted properties of the 18 compounds. This material is available free of charge via the Internet at http://pubs.acs.org.

AUTHOR INFORMATION

Corresponding Author

*E-mail: huangjin@ecust.edu.cn (J.H.); hlli@ecust.edu.cn (H.L.). Phone/fax: +86-21-64250213 (H.L.).

Author Contributions

[†]These authors contributed equally to this work.

Notes

The authors declare no competing financial interest.

ACKNOWLEDGMENTS

This work was supported by the Fundamental Research Funds for the Central Universities, the National Natural Science Foundation of China (grants 21173076, 81102375, 10979072, 81222046, and 81230076), the Specialized Research Fund for the Doctoral Program of Higher Education of China (grants

20090074120012 and 20110074120009), the Special Fund for Major State Basic Research Project (grant 2009CB918501), the Shanghai Committee of Science and Technology (grants 11DZ2260600 and 10431902600), and the 863 Hi-Tech Program of China (grant 2012AA020308). Honglin Li is also sponsored by Program for New Century Excellent Talents in University (grant NCET-10-0378).

■ ABBREVIATIONS USED

*h*DHODH, human dihydroorotate dehydrogenase; *pf*DHODH, *Plasmodium falciparum* DHODH; DHO, dihydroorotate; FMN, flavin mononucleotide; rmsd, root-mean-square deviation; VDW, van der Waals; Tc, Tanimoto coefficients; DCIP, 2,6-dichloroindophenol; LPS, lipopolysaccharide; MLR, mixed lymphocyte reaction; CsA, cyclosporin A

■ REFERENCES

(1) Palfey, B. A.; Björnberg, O.; Jensen, K. F. Insight into the chemistry of flavin reduction and oxidation in *Escherichia coli* dihydroorotate dehydrogenase obtained by rapid reaction studies. *Biochemistry* **2001**, *40* (14), 4381−4390.

(2) Nagy, M.; Lacroute, F.; Thomas, D. Divergent evolution of pyrimidine biosynthesis between anaerobic and aerobic yeasts. *Proc. Natl. Acad. Sci. U.S.A.* **1992**, *89* (19), 8966−8970.

(3) Kulkarni, O. P.; Sayyed, S. G.; Kantner, C.; Ryu, M.; Schnurr, M.; Sardy, M.; Leban, J.; Jankowsky, R.; Ammendola, A.; Doblhofer, R. 4SC-101, a novel small molecule dihydroorotate dehydrogenase inhibitor, suppresses systemic lupus erythematosus in MRL-(Fas) lpr mice. *Am. J. Pathol.* **2010**, *176* (6), 2840−2847.

(4) Gummert, J.; Ikonen, T.; Morris, R. Newer immunosuppressive drugs: a review. *J. Am. Soc. Nephrol.* **1999**, *10* (6), 1366−1380.

(5) Löffler, M.; Fairbanks, L.; Zameitat, E.; Marinaki, A.; Simmonds, H. Pyrimidine pathways in health and disease. *Trends Mol. Med.* **2005**, *11* (9), 430−437.

(6) Khutornenko, A. A.; Roudko, V. V.; Chernyak, B. V.; Vartapetian, A. B.; Chumakov, P. M.; Evstafieva, A. G. Pyrimidine biosynthesis links mitochondrial respiration to the p53 pathway. *Proc. Natl. Acad. Sci. U.S.A.* **2010**, *107* (29), 12828−12833.

(7) Hoffmann, H. H.; Kunz, A.; Simon, V. A.; Palese, P.; Shaw, M. L. Broad-spectrum antiviral that interferes with de novo pyrimidine biosynthesis. *Proc. Natl. Acad. Sci. U.S.A.* **2011**, *108* (14), 5777.

(8) Wang, Q. Y.; Bushell, S.; Qing, M.; Xu, H. Y.; Bonavia, A.; Nunes, S.; Zhou, J.; Poh, M. K.; de Sessions, P. F.; Niyomrattanakit, P. Inhibition of dengue virus through suppression of host pyrimidine biosynthesis. *J. Virol.* **2011**, *85* (13), 6548−6556.

(9) Hansen, M.; Le Nours, J.; Johansson, E.; Antal, T.; Ullrich, A.; Löffler, M.; Larsen, S. Inhibitor binding in a class 2 dihydroorotate dehydrogenase causes variations in the membrane-associated N-terminal domain. *Protein Sci.* **2004**, *13* (4), 1031−1042.

(10) DeFrees, S. A.; Sawick, D. P.; Cunningham, B.; Heinstein, P. F.; James Morré, D.; Cassady, J. M. Structure-activity relationships of pyrimidines as dihydroorotate dehydrogenase inhibitors. *Biochem. Pharmacol.* **1988**, *37* (20), 3807−3816.

(11) Baumgartner, R.; Walloschek, M.; Kralik, M.; Gotschlich, A.; Tasler, S.; Mies, J.; Leban, J. Dual binding mode of a novel series of DHODH inhibitors. *J. Med. Chem.* **2006**, *49* (4), 1239−1247.

(12) Fritzson, I.; Svensson, B.; Al-Karadaghi, S.; Walse, B.; Wellmar, U.; Nilsson, U.; da Gra a Thrige, D.; Jönsson, S. Inhibition of human DHODH by 4-hydroxycoumarins, fenamic acids, and N-(alkylcarbonyl) anthranilic acids identified by structure-guided fragment selection. *ChemMedChem* **2010**, *5* (4), 608−617.

(13) Davies, M.; Heikkila, T.; McConkey, G. A.; Fishwick, C. W. G.; Parsons, M. R.; Johnson, A. P. Structure-based design, synthesis, and characterization of inhibitors of human and *Plasmodium falciparum* dihydroorotate dehydrogenases. *J. Med. Chem.* **2009**, *52* (9), 2683−2693.

(14) Rückemann, K.; Fairbanks, L.; Carrey, E.; Hawrylowicz, C.; Richards, D.; Kirschbaum, B.; Simmonds, H. Leflunomide inhibits pyrimidine de novo synthesis in mitogen-stimulated T-lymphocytes from healthy humans. *J. Biol. Chem.* **1998**, *273* (34), 21682−21691.

(15) White, R. M.; Cech, J.; Ratanasirintrawoot, S.; Lin, C. Y.; Rahl, P. B.; Burke, C. J.; Langdon, E.; Tomlinson, M. L.; Mosher, J.; Kaufman, C. DHODH modulates transcriptional elongation in the neural crest and melanoma. *Nature* **2011**, *471* (7339), 518−522.

(16) Alcorn, N.; Saunders, S.; Madhok, R. Benefit-risk assessment of leflunomide. *Drug Saf.* **2009**, *32* (12), 1123−1134.

(17) Suissa, S.; Hudson, M.; Ernst, P. Leflunomide use and the risk of interstitial lung disease in rheumatoid arthritis. *Arthritis Rheum.* **2006**, *54* (5), 1435−1439.

(18) Maroun, J.; Ruckdeschel, J.; Natale, R.; Morgan, R.; Dallaire, B.; Sisk, R.; Gyves, J. Multicenter phase II study of brequinar sodium in patients with advanced lung cancer. *Cancer Chemother. Pharmacol.* **1993**, *32* (1), 64−66.

(19) Pally, C.; Smith, D.; Jaffee, B.; Magolda, R.; Zehender, H.; Dorobek, B.; Donatsch, P.; Papageorgiou, C.; Schuurman, H. J. Side effects of brequinar and brequinar analogues, in combination with cyclosporine, in the rat. *Toxicology* **1998**, *127* (1−3), 207−222.

(20) Knecht, W.; Henseling, J.; Löffler, M. Kinetics of inhibition of human and rat dihydroorotate dehydrogenase by atovaquone, lawsone derivatives, brequinar sodium and polyporic acid. *Chem.-Biol. Interact.* **2000**, *124* (1), 61−76.

(21) Vyas, V. K.; Ghate, M. Recent developments in the medicinal chemistry and therapeutic potential of dihydroorotate dehydrogenase (DHODH) inhibitors. *Mini-Rev. Med. Chem.* **2011**, *11* (12), 1039−1055.

(22) Liu, S.; Neidhardt, E.; Grossman, T.; Ocain, T.; Clardy, J. Structures of human dihydroorotate dehydrogenase in complex with antiproliferative agents. *Structure* **2000**, *8* (1), 25−33.

(23) Kitchen, D.; Decornez, H.; Furr, J.; Bajorath, J. Docking and scoring in virtual screening for drug discovery: methods and applications. *Nat. Rev. Drug Discovery* **2004**, *3* (11), 935−949.

(24) Berman, H. M.; Westbrook, J.; Feng, Z.; Gilliland, G.; Bhat, T.; Weissig, H.; Shindyalov, I. N.; Bourne, P. E. The protein data bank. *Nucleic Acids Res.* **2000**, *28* (1), 235−242.

(25) *Schrödinger Suite 2009 Protein Preparation Wizard*; Epik version 2.0, Schrödinger, LLC, New York, NY, 2009; Impact version 5.5, Schrödinger, LLC, New York, NY, 2009; Prime version 2.1, Schrödinger, LLC, New York, NY, 2009.

(26) Friesner, R.; Banks, J.; Murphy, R.; Halgren, T.; Klicic, J.; Mainz, D.; Repasky, M.; Knoll, E.; Shelley, M.; Perry, J. Glide: a new approach for rapid, accurate docking and scoring. 1. Method and assessment of docking accuracy. *J. Med. Chem.* **2004**, *47* (7), 1739−1749.

(27) Halgren, T.; Murphy, R.; Friesner, R.; Beard, H.; Frye, L.; Pollard, W.; Banks, J. Glide: a new approach for rapid, accurate docking and scoring. 2. Enrichment factors in database screening. *J. Med. Chem.* **2004**, *47* (7), 1750−1759.

(28) Specs: Chemistry Solutions for Drug Discovery. http://www.specs.net/ (accessed March 1, 2010).

(29) *LigPrep*, version 2.0; Schrödinger, LLC, New York, NY, 2005.

(30) Yu, Z.; Jacobson, M. P.; Friesner, R. A. What role do surfaces play in GB models? A new generation of surface-generalized born model based on a novel gaussian surface for biomolecules. *J. Comput. Chem.* **2006**, *27* (1), 72−89.

(31) *Prime*, version 2.1; Schrödinger, LLC, New York, NY, 2009.

(32) *Pipeline Pilot*, version 7.5; Accelrys, San Diego, CA, 2008.

(33) Rogers, D.; Hahn, M. Extended-connectivity fingerprints. *J. Chem. Inf. Model.* **2010**, *50* (5), 742−754.

(34) Patel, V.; Booker, M.; Kramer, M.; Ross, L.; Celatka, C. A.; Kennedy, L. M.; Dvorin, J. D.; Duraisingh, M. T.; Sliz, P.; Wirth, D. F. Identification and characterization of small molecule inhibitors of Plasmodium falciparum dihydroorotate dehydrogenase. *J. Biol. Chem.* **2008**, *283* (50), 35078−35085.

(35) Boa, A. N.; Canavan, S. P.; Hirst, P. R.; Ramsey, C.; Stead, A. M. W.; McConkey, G. A. Synthesis of brequinar analogue inhibitors of

malaria parasite dihydroorotate dehydrogenase. *Bioorg. Med. Chem. Lett.* **2005**, *13* (6), 1945−1967.
(36) Li, J.; Chen, J.; Zhang, L.; Wang, F.; Gui, C.; Qin, Y.; Xu, Q.; Liu, H.; Nan, F.; Shen, J. One novel quinoxaline derivative as a potent human cyclophilin A inhibitor shows highly inhibitory activity against mouse spleen cell proliferation. *Bioorg. Med. Chem.* **2006**, *14* (16), 5527−5534.
(37) Fehr, T.; Kallen, J.; Oberer, L.; Sanglier, J. J.; Schilling, W. Sanglifehrins A, B, C and D, novel cyclophilin-binding compounds isolated from Streptomyces sp. A92-308110. II. Structure elucidation, stereochemistry and physico-chemical properties. *J. Antibiot.* **1999**, *52* (5), 466−473.
(38) McLean, L.; Zhang, Y.; Degnen, W.; Peppard, J.; Cabel, D.; Zou, C.; Tsay, J.; Subramaniam, A.; Vaz, R.; Li, Y. Discovery of novel Inhibitors for DHODH via virtual screening and X-ray crystallographic structures. *Bioorg. Med. Chem. Lett.* **2010**, *20* (6), 1981−1984.
(39) Hurt, D.; Sutton, A.; Clardy, J. Brequinar derivatives and species-specific drug design for dihydroorotate dehydrogenase. *Bioorg. Med. Chem. Lett.* **2006**, *16* (6), 1610−1615.
(40) Walse, B.; Dufe, V.; Svensson, B.; Fritzson, I.; Dahlberg, L.; Khairoullina, A.; Wellmar, U.; Al-Karadaghi, S. The structures of human dihydroorotate dehydrogenase with and without inhibitor reveal conformational flexibility in the inhibitor and substrate binding sites. *Biochemistry* **2008**, *47* (34), 8929−8936.
(41) David, L.; Ken, A. Binding of small-molecule ligands to proteins: "what you see" is not always "what you get". *Structure* **2009**, *17*, 489−498.
(42) Lyne, P. D.; Lamb, M. L.; Saeh, J. C. Accurate prediction of the relative potencies of members of a series of kinase inhibitors using molecular docking and MM-GBSA scoring. *J. Med. Chem.* **2006**, *49* (16), 4805−4808.
(43) Massova, I.; Kollman, P. A. Combined molecular mechanical and continuum solvent approach (MM-PBSA/GBSA) to predict ligand binding. *Perspect. Drug Discovery* **2000**, *18* (1), 113−135.
(44) Carlsson, J.; Coleman, R. G.; Setola, V.; Irwin, J. J.; Fan, H.; Schlessinger, A.; Sali, A.; Roth, B. L.; Shoichet, B. K. Ligand discovery from a dopamine D3 receptor homology model and crystal structure. *Nat. Chem. Biol.* **2011**, *7* (11), 769−778.
(45) Holla, B. S.; Malini, K.; Rao, B. S.; Sarojini, B.; Kumari, N. S. Synthesis of some new 2,4-disubstituted thiazoles as possible antibacterial and anti-inflammatory agents. *Eur. J. Med. Chem.* **2003**, *38* (3), 313−318.
(46) Karegoudar, P.; Karthikeyan, M. S.; Prasad, D. J.; Mahalinga, M.; Holla, B. S.; Kumari, N. S. Synthesis of some novel 2,4-disubstituted thiazoles as possible antimicrobial agents. *Eur. J. Med. Chem.* **2008**, *43* (2), 261−267.
(47) Baldwin, J.; Farajallah, A. M.; Malmquist, N. A.; Rathod, P. K.; Phillips, M. A. Malarial dihydroorotate dehydrogenase. *J. Biol. Chem.* **2002**, *277* (44), 41827−41834.
(48) Li, H.; Huang, J.; Chen, L.; Liu, X.; Chen, T.; Zhu, J.; Lu, W.; Shen, X.; Li, J.; Hilgenfeld, R. Identification of novel falcipain-2 inhibitors as potential antimalarial agents through structure-based virtual screening. *J. Med. Chem.* **2009**, *52* (15), 4936−4940.
(49) Hurt, D. E.; Widom, J.; Clardy, J. Structure of Plasmodium falciparum dihydroorotate dehydrogenase with a bound inhibitor. *Acta Crystallogr., Sect. D: Biol. Crystallogr.* **2006**, *62* (3), 312−323.
(50) Phillips, M.; Rathod, P. Plasmodium dihydroorotate dehydrogenase: a promising target for novel anti-malarial chemotherapy. *Infect. Disorders - Drug Targets* **2010**, *10* (3), 226−239.
(51) Davidson, A.; Diamond, B. Autoimmune diseases. *N. Engl. J. Med.* **2001**, *345* (5), 340−350.
(52) Dimitrova, P.; Kalden, J. R.; Schulze-Koops, H. Leflunomide: an immunosuppressive drug with multiple effects on T cell function. *Mod. Rheumatol.* **2002**, *12* (3), 195−200.
(53) Herrmann, M. L.; Schleyerbach, R.; Kirschbaum, B. J. Leflunomide: an immunomodulatory drug for the treatment of rheumatoid arthritis and other autoimmune diseases. *Immunopharmacology* **2000**, *47* (2−3), 273−289.
(54) Papageorgiou, C.; von Matt, A.; Joergensen, J.; Andersen, E.; Wagner, K.; Beerli, C.; Than, T.; Borer, X.; Florineth, A.; Rihs, G. Aromatic quinolinecarboxamides as selective, orally active antibody production inhibitors for prevention of acute xenograft rejection. *J. Med. Chem.* **2001**, *44* (12), 1986−1992.
(55) Papageorgiou, C.; Albert, R.; Floersheim, P.; Lemaire, M.; Bitch, F.; Weber, H. P.; Andersen, E.; Hungerford, V.; Schreier, M. H. Pyrazole bioisosteres of leflunomide as B-cell immunosuppressants for xenotransplantation and chronic rejection: scope and limitations. *J. Med. Chem.* **1998**, *41* (18), 3530−3538.